TERMS OF USE
This pdf is provided by Magnolia Press for private/research use.
Commercial sale or deposition in a public library or website is prohibited.

Zootaxa 3731 (1): 153–170
www.mapress.com/zootaxa/
Copyright © 2013 Magnolia Press

Article

ISSN 1175-5326 (print edition)
ZOOTAXA
ISSN 1175-5334 (online edition)

http://dx.doi.org/10.11646/zootaxa.3731.1.7
http://zoobank.org/urn:lsid:zoobank.org:pub:15283247-C6B3-42E3-970F-6C7068994467

Odontobuthus tirgari sp. nov. (Scorpiones, Buthidae) from the eastern region of the Iranian Plateau

OMID MIRSHAMSI[1,2]*, SARA AZGHADI[1], SHAHROKH NAVIDPOUR[3], MANSOUR ALIABADIAN[1,2] & FRANTIŠEK KOVAŘÍK[4]

[1]*Department of Biology, Faculty of Sciences, Ferdowsi University of Mashhad, Mashhad, Iran*
[2]*Zoological Innovations Research Department, Institute of Applied Zoology, Faculty of Sciences, Ferdowsi University of Mashhad, Mashhad, Iran*
[3]*Razi Reference Laboratory of Scorpion Research, Razi Vaccine and Serum Research Institute, P.O. Box 31975/148, Department of Venomous Animals & Toxins, Hesarak, Karaj, Iran*
[4]*P.O. Box 27, CZ-145 01 Praha 45, Czech Republic; www.kovarex.com/scorpio*
**Corresponding author: mirshams@ferdowsi.um.ac.ir*

Abstract

A new species of scorpions in the genus *Odontobuthus* (Scorpiones, Buthidae) is described from Khorasan Province, Iran. Currently, *Odontobuthus* includes two species in Iran, *Odontobuthus doriae* Thorell, 1876, which is restricted to high elevations of the central Iranian Plateau and *Odontobuthus bidentatus* Lourenço & Pezier, 2002 from the Zagros Mountains. The results of morphological comparisons, univariate and multivariate statistical analyses and phylogenetic analysis of *COI* sequence data clearly confirm a deep split between populations from the eastern Iranian Plateau and *O. bidentatus* Lourenço & Pezier, 2002 and *O. doriae* Thorell, 1876. Therefore, according to comparative morphological and molecular analyses, a new species, *Odontobuthus tigari* sp. nov. (♀♂) was described from eastern Iran. This addition represents the third species of this genus from Iran.

Key words: Scorpion, fauna, Khorasan, new species, *COI*

Introduction

In 1950, Dr. Max Vachon at the Museum National d'Histoire Naturelle, France, created a new buthid genus named *Odontobuthus* after his revision of the traditional genus *Buthus* Leach, 1815. He partitioned this large taxon into several genera primarily based on differences in carination of prosoma, tergites and metasomal segments. The genus *Odontobuthus* is characterized by sharing prominent, enlarged dentition on metasomal segments II–III. Vachon (1950) considered *O. doriae* and *O. odonturus* as distinct species, *O. doriae* which was recorded from high elevations of western and central Iran and *O. odonturus* from the Indus River drainage of eastern Pakistan and the Rajasthan desert of western India. Lourenço & Pézier (2002) confirmed the taxonomic validity of these taxa as separate species in their revision of the genus *Odontobuthus*. They also described the third species, namely *O. bidentatus* from the Tigris-Euphrates River drainage of eastern Iraq and the western foothills of the Zagros Mountains in Iran. Lowe (2010) described the fourth species, *O. brevidigitus*, from northern Oman. The discovery of this species represents a significant range extension of this genus across the Persian Gulf into the Arabian Peninsula (Lowe, 2010). All *Odontobuthus* species are fossorial animals with distinct morphological adaptations for burrowing in consolidated sandy or silty substrates on alluvial plains (Lowe, 2010; Farzanpay, 1987). The genus *Odontobuthus* is known by two species in Iran, namely, *O. doriae* and *O. bidentatus* (Lourenço & Pézier, 2002; Navidpour et al., 2008a,b,c,d; Lowe, 2010). All of the previous records of *O. odonturus* from Iran (Farzanpay, 1987; Kovařík, 1997) are now considered as *O. bidentatus* (Lourenço & Pézier, 2002), therefore, the record of *O. odonturus* from Iran requires further investigations.

Systematic studies on the scorpion fauna have not been performed intensively in much of central, eastern and southern Iran because of lacking comprehensive sampling from the distribution ranges of *Odontobuthus*. Therefore, confirmed records of the genus *Odontobuthus* in eastern parts of Iran are lacking. For example, Birula

Accepted by L. Prendini: 9 Oct.2013; published: 29 Oct. 2013

TERMS OF USE
This pdf is provided by Magnolia Press for private/research use.
Commercial sale or deposition in a public library or website is prohibited.

(1900, 1905) refers to several records of *O. odonturus* from southeast of Iran, but these records have not been reviewed and the relationships between these forms and western (*O. doriae*) and eastern (*O. odonturus*) are unclear. In this study, the taxonomic validity and relationships of the Iranian species of the genus *Odontobuthus* and the taxonomic status of the populations from eastern parts of Iran were evaluated using statistical analyses of morphological data and the analysis of cytochrome C oxidase, subunit I (*COI*) sequence data.

Material and Methods

Sampling

Specimens were collected using ultraviolet light detection at night and excavation of burrows during the day. All material was transferred into 75–96% alcohol and deposited in the scorpion collection at the Zoological Museum, Ferdowsi University of Mashhad (ZMFUM), Mashhad, Iran; František Kovařík Collection (FKCP), Praha, Czech Republic and American Museum of Natural History (AMNH), New York, USA.

Morphological studies

Examination of cuticular sculpture and morphology was facilitated using ultraviolet fluorescence photomicrography by LED excitation source (Lowe et al. 2003; Prendini 2004; Volschenk 2005; Lowe 2010) and photographs were taken with epifluorescence technique (Lowe et al. 2003). Illustrations were produced using a camera lucida fitted on an Olympus SZH-10 stereomicroscope**.** Morphometric measurements were taken with a >0.02 mm accurate micrometric ocular lens applied to an optical Olympus SZ40 stereomicroscope. Following methods applied by Lamoral (1979) and Stahnke (1970), measurements of 27 morphometric characters of adult *Odontobuthus* specimens were used in the subsequent statistical analysis. The morphological nomenclatures were adapted from Sissom (1990).

Data analysis using standard statistical methods, principal component and canonical discriminant analyses were performed within SPSS version 13 and PAST statistical packages (Hammer et al. 2001). Since Levene's test revealed that almost all variables lacked an assumption of variance homogeneity, logarithmic transformation of data was used in multivariate statistical analyses.

Laboratory methods

DNA was isolated from scorpion muscle tissue, using the GenNetBio™ genomic DNA Extraction kit following the manufacturer's protocol (Seoul, South Korea). Polymerase chain reaction (PCR) was subsequently performed to amplify approximately 700 base pairs (bp) of the mitochondrial cytochrome C oxidase, subunit I (*COI*) gene. Primers used include LCO1490 (Folmer et al. 1994) and Nancy (Simon et al. 1994). Each PCR master mix contained 2.5 µl 10 × PCR buffer (100 mM Tris–HCl pH 8.3, 1.5 mM MgCl2, 500 mM KCl), 2 µl dNTP mix (2.5 mM of each dNTP); 0.6 µl (= 6 pmol) of each primer, 0.125 µl *Taq* DNA polymerase (5 units/µl, Takara Bio Inc., Shiga, Japan), and 1–5 µl DNA template. We used the following PCR thermal regimen: one cycle of 2.5 min at 94°C; five cycles of 45s at 94°C, 45s at 45°C, and 1 min at 72°C; 35 cycles of 45 seconds at 94°C, 1 min at 51°C, and 1 min at 72°C; and a final cycle of 10 min at 72°C. Sequencing was performed using ABI Big Dye terminator and an ABI Prism 3700 instrument (Applied Biosystems, Foster City, CA, USA). Sequences were analyzed in SEQUENCHER version 4.1.1 (GeneCodes Corporation, Ann Arbor, MI, USA).

Phylogenetic Analyses

Sequence alignment was performed using CLUSTALX program (version 1.8, Thompson et al. 1997). All new *COI* sequences were deposited in GenBank [http://www.ncbi.nlm.nih.gov with the accession numbers KF701308 to KF701322].

DNASP 5 (Rozas et al. 2003), MEGA4 (Tamura et al. 2007) and ExCaliBAR (Aliabadian et al. in press) softwares were used to compare sequence characterizations, nucleotide diversities and levels of divergence between *O. doriae, O. bidentatus, Odontobuthus tirgari* sp. nov., and the outgroup species *Androctonus crassicauda* Oliver, 1897 (Buthidae). As suggested from morphological analyses, the buthid species *A. australis* (Linnaeus, 1758) is an ideal outgroup, and has been frequently used as outgroup in phylogenetic studies (Gantenbein and Largiadèr 2003; Gantenbein et al. 2003; Parmakelis et al. 2006). Therefore, the Old World buthid, *Androctonus crassicauda* (Olivier, 1807) was used as outgroup in the present study.

TERMS OF USE
This pdf is provided by Magnolia Press for private/research use.
Commercial sale or deposition in a public library or website is prohibited.

For maximum likelihood analyses, the best substitution model was selected with jMODELTEST (version 0.1.1, Posada 2005). Parameters from this best model were used for subsequent maximum likelihood analyses in PAUP with 100 random stepwise additions and TBR branch swapping. Support was determined using a 500 bootstrap analysis. A Bayesian analysis was performed in MrBayes (version 3.2, Ronquist and Huelsenbeck, 2003) using the same substitution model selected for the ML analysis. The number of generations was set to 2.5×10^6 and a tree was sampled every 100th generation. The average standard deviation of split frequencies of the two simultaneous and independent runs performed by Mrbayes 3.2 was used to determine the stationary point of likelihoods (Ronquist and Huelsenbeck, 2003). Bayesian topology and posterior probabilities were computed by majority rule consensus after burning of all pre-asymptotic trees.

Abbreviations

Specimen depositories: ZMFUM, Zoological Museum Ferdowsi University of Mashhad, Mashhad, Iran. FKCP, František Kovařík Collection Praha, Czech Republic; AMNH, American Museum of Natural History, New York, USA.

Morphometric variables: BL: body length; CL: carapace length; CWA: anterior width of carapace; CWP: posterior width of carapace; X: distance between anterior margin of carapace and anterior margin of median eyes; Y: distance between anterior margin of median eyes and posterior margin of carapace; Mt(I–V)L: length of metasomal segments I–V; Mt (I–V)W: width of metasomal segments I–V; Mt (I–V)H: height of metasomal segments I–V; TlL: telson length; TlW: telson width; TlH: telson height; ChL: chela length; ML: manus length; MFL: movable finger length.

Results

The results of the morphological examinations clearly revealed that the samples from eastern regions of Iran are significantly different from other species of the genus *Odontobuthus* described from Iran. These samples are consistently distinguishable from other species by a combination of the following morphological characteristics: smaller body size, presence of three lobes on the lateral anal arch, lacking enlarged triangular denticles on the ventral anal arch, transverse row of eight or more enlarged granules on the metasomal segment IV and 12–13 oblique rows of granules on movable finger of pedipalp. Therefore, a new morphological species, *O. tirgari* sp. nov., was proposed and its taxonomic validity was evaluated using uni- and multivariate statistical analyses and phylogenetic analysis of *COI* mtDNA sequences.

Statistical results. The results of T^2 Hotelling discriminant analysis based on males and females showed a significant difference between sexes ($P<0.05$). Therefore, because of small sample size of males, subsequent statistical analyses were performed only on the female dataset. Generally, adult males are smaller (66.37±1.22 mm) than females (70.75±0.77 mm) and bear a higher number of pectinal teeth (31|30; left|right) than females (20|19; left|right), and thus show longer pectines. Moreover, the metasomal segments in males are longer than females with same total body length.

The descriptive statistics (mean±SE) and the results of Kruskall-Wallis one-way ANOVA of morphometric characters and ratios for each identified species of the genus *Odontobuthus* were calculated (Table 1). Evaluation of morphological differences for each species showed that the studied species are different based on the mean values for each variable. The results of univariate comparisons (Table 1) showed that all of the mean values in *O. tirgari* sp. nov., except MFL, are smaller than those for *O. doriae* and *O. bidentatus*. Moreover, the results of Kruskall-Wallis ANOVA revealed significant difference among all measured morphometric characters, except for Mt(I)L (Table 1).

Four principal components are presented while the total eigenvalue is 0.0277, and the total of the four components explain 89.64% of the accumulated variance (Table 2). However, the scatterplot for the first and second components (PC_1 *vs.* PC_2) showed a separation along the first component between the eastern species, *O. tirgari* sp. nov., and other two species, *O. doriae* and *O. bidentatus* (Fig. 1). *O. tirgari* sp. nov. scores are separated and are higher along PC_1 than other *Odontobuthus* species. These observations are consistent with PC_1 being correlated with overall size (Table 1), *O. tirgari* sp. nov. is smaller than other species. Moreover, *O. doriae* scores

TERMS OF USE
This pdf is provided by Magnolia Press for private/research use.
Commercial sale or deposition in a public library or website is prohibited.

are lower along PC_2 than other species, suggesting morphological differences between these groups. The loadings for PC2 (Table 2) mainly emphasize the different shapes of metasomal segments I, II and IV, telson and pedipalp chela in *O. tirgari* and *O. doriae*.

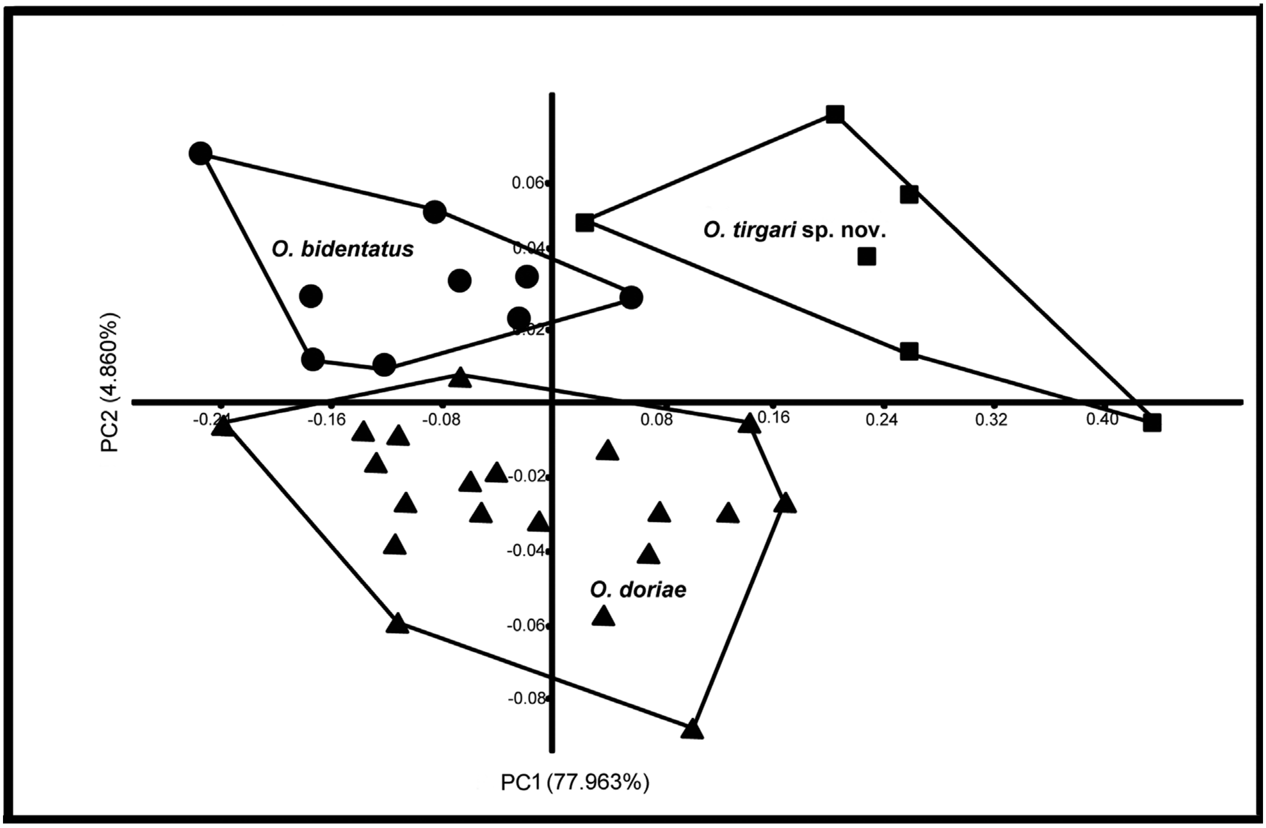

FIGURE 1. Principal component analysis of the genus *Odontobuthus* based on 27 morphometric characters for the first (PC_1) and second (PC_2) components. The scatterplot indicates the separation of *Odontobuthus tirgari* sp. nov. with respect to *O. doriae* and *O. bidentatus* along the first and second principal components.

Stepwise discriminant analysis using Mahalanobis distance for *Odontobuthus* species demonstrated that all examined *Odontobuthus* species formed three well defined phenetic groups: *O. doriae, O. bidentatus* and *O. tirgari* sp. nov.. The resulting scatterplot clearly indicates the distinction of *O. tirgari* sp. nov. from other species along Function 1(Fig. 2). Along the horizontal axis (Function 1) ML and MFL have the larger absolute value of function coefficient and have the larger ability to discriminate *O. tirgari* sp. nov. from other species. In this analysis, when four morphometric variables were entered (*i.e.* ML, MFL, Mt(IV)W and TlH), Wilk's λ dropped to 0.054 with a significant difference among defined groups (F=23.754, P <0.001).

Molecular results. In total, the *COI* gene was sequenced for 14 individuals of the genus *Odontobuthus,* including five *O. dorie*, four *O. bidentatus* and five *O. tirgari* sp. nov. and one specimen of *Androctonus crassicauda*. The final multiple sequence alignment of *Odontobuthus* species and the outgroup species (*A. crassicauda*) includes 674 bp of which, 535 bp (79.37%) were conserved, 136 bp (20.17%) were polymorphic and 82 bp (12.16%) were parsimony informative. Overall nucleotide (π) and haplotype diversity within *Odontobuthus* were 0.088 and 0.92, respectively.

The best-fit model of sequence evolution for *COI* determined by jMODELTEST 0.1 .1 under Akaike information criterion (AIC) was TIM3+G (-*ln*L = 1564.3730; Akaike information criterion 3202.7145). Estimates for the model parameters employed in maximum likelihood searches included estimated base frequencies (πA = 0.1927, πC = 0.1333, πG = 0.2593, πT = 0.4147), rate parameter estimates ([A< >C] = 0.0000; [A< >G] = 12.9951; [A< >T] = 1.0000; [C< >G] = 0.0000; [C< >T] = 1.5342; [G< >T] = 1.0000), and gamma distribution shape parameter (α = 0.2580).

TERMS OF USE
This pdf is provided by Magnolia Press for private/research use.
Commercial sale or deposition in a public library or website is prohibited.

Phylogenies produced using maximum likelihood and Bayesian inference methods produced congruent topologies. The resulting trees all predicted the existence of three clades with high nodal support: *O. doriae* (*doriae* clade: bootstrap value = 99%; posterior probability = 100) from central Iranian Plateau; *O. bidentatus* (*bidentatus* clade: bootstrap value = 99%; posterior probability = 100) from Zagros Mountains; and *O. tirgari* sp. nov. (*tirgari* clade: bootstrap value=100; Posterior probability= 100) from the eastern Iranian Plateau (Fig. 3). The resulting topology suggested a sister relationship between *O. tirgari* sp. nov. and *O. bidentatus*, however, this relationship received low nodal support (bootstrap value = 72%).

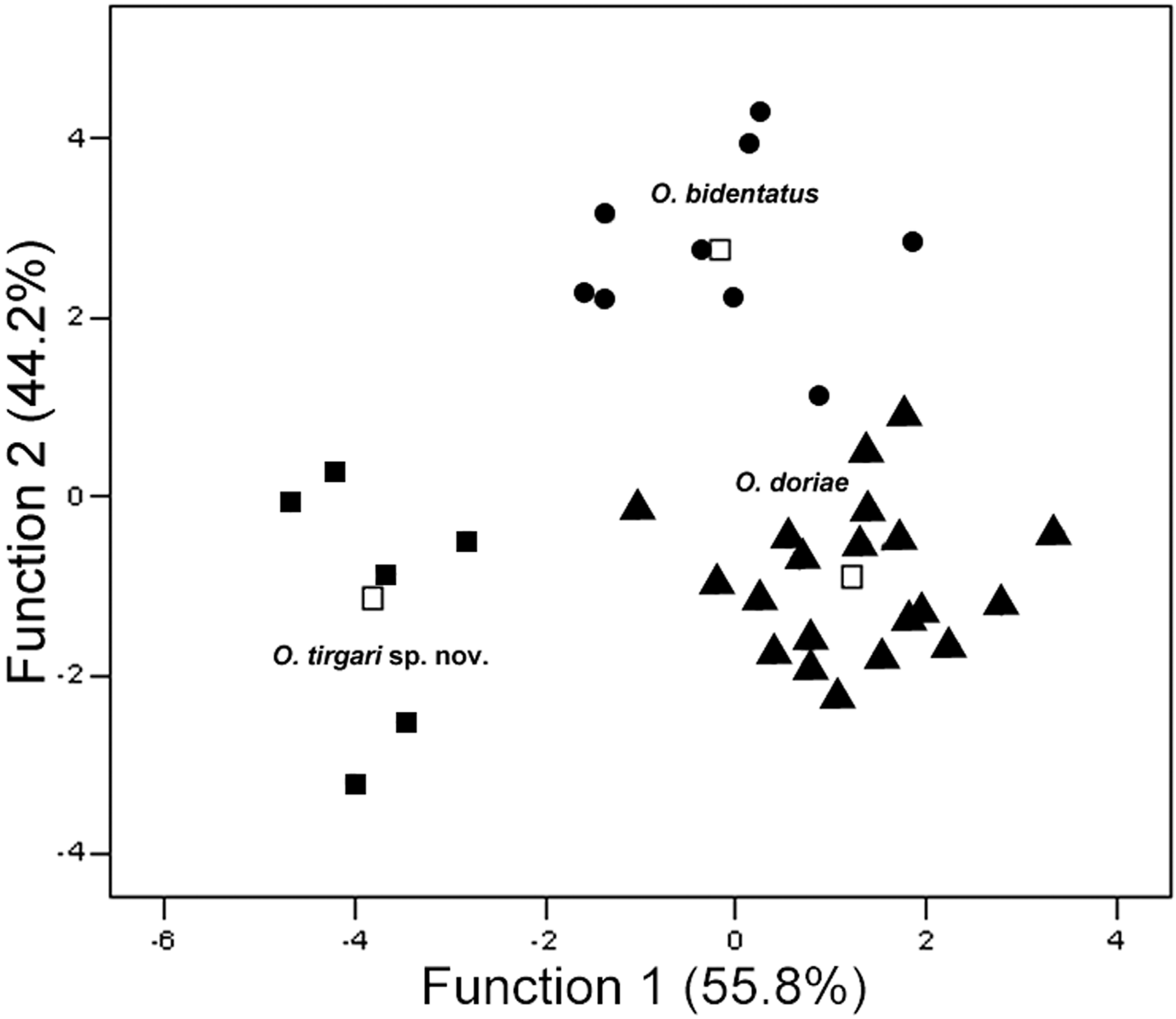

FIGURE 2. Canonical discriminant analysis of *Odontobuthus* species based on 27 morphometric characters. (■): *Odontobuthus tirgari* sp. nov.; (▲): *O. doriae*; (●): *O. bidentatus*; (□): Group centroid.

Genetic distances among the resulting *Odontobuthus* clades and *A. crassicauda* were calculated. K2P and net between averages were used in the calculations. The K2P genetic distances among *Odontobuthus* species ranged between 10% and 12% and the maximum distance was observed between *O. doriae* and *O. tirgari* sp. nov. (i.e. 12%). The mean intraspecific genetic distance within the genus *Odontobuthus* is 0.005± 0.001.The distances between each *Odontobuthus* species and *A. crassicauda* ranged from 15% to 16%.

TERMS OF USE
This pdf is provided by Magnolia Press for private/research use.
Commercial sale or deposition in a public library or website is prohibited.

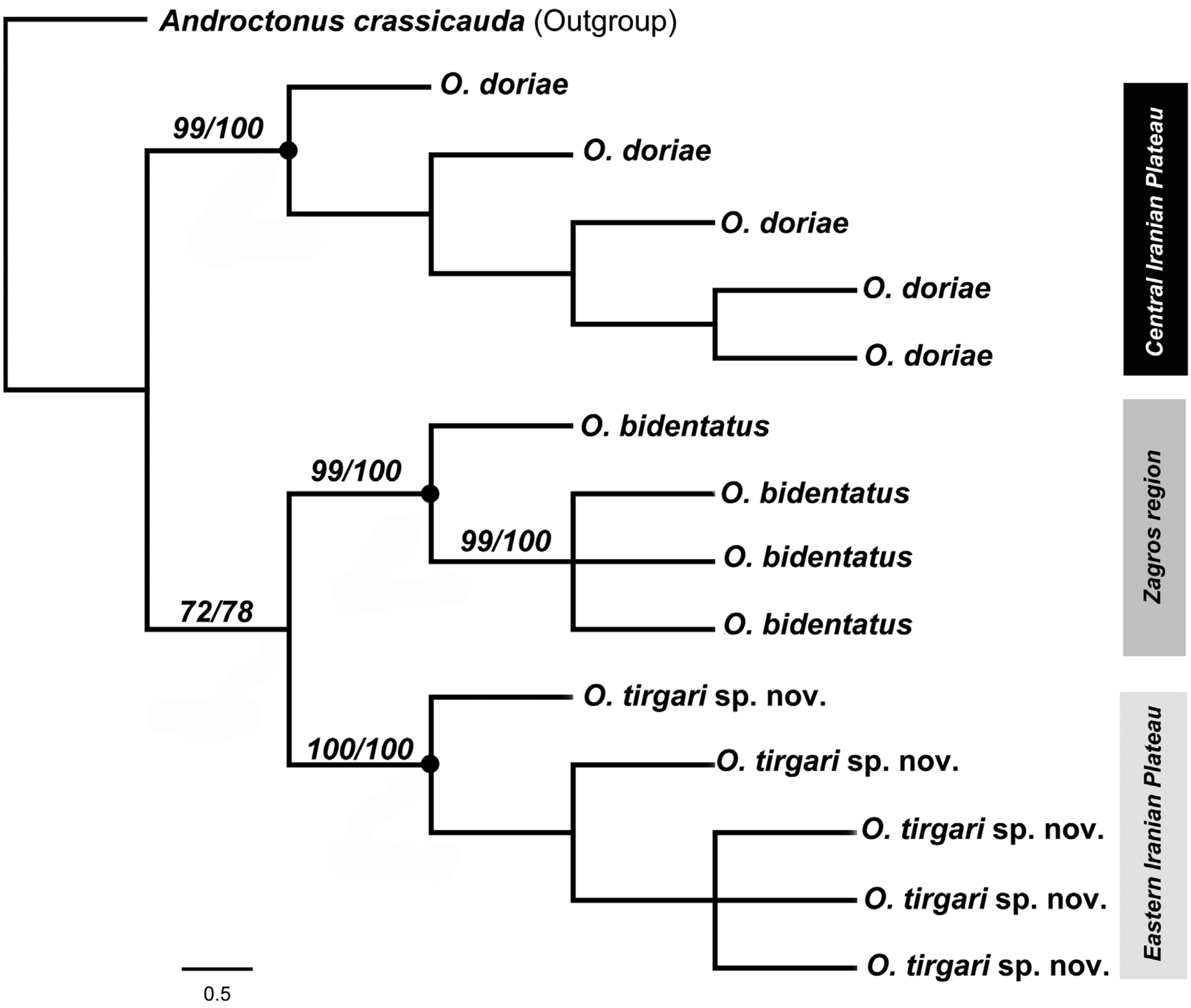

FIGURE 3. Fifty percent majority rule consensus tree resulting from maximum likelihood and Bayesian analyses. Numbers above branches are the bootstrap values (left) and posterior probabilities (right) of the nodes in the maximum likelihood and Bayesian inference analyses, respectively.

Systematics

The major finding of the present study, based on the results of morphological characters, multivariate statistical analysis of specimens and the analysis of *COI* sequence data is that the eastern populations of the genus *Odontobuthus* can be classified separately from *O. doriae* and *O. bidentatus*. This provides support for describing the eastern populations (*O. tirgari*) as a novel species. Therefore, we provide detailed descriptions for *Odontobuthus tirgari* sp. nov., which is morphologically and genetically distinct from other species.

Genus *Odontobuthus* Vachon, 1950

Type is *Buthus doriae* Thorell, 1877.

Odontobuthus tirgari sp. nov.

Figs. 4–30, Table 1

Type material: *Holotype* **:** ♀, Iran, Khorasan Province, Gonabad, ca. 5 km NE of Kakhk, daytime excavation, 1 September 2007, leg. O. Mirshamsi (ZMFUM-scr-2120).

TERMS OF USE
This pdf is provided by Magnolia Press for private/research use.
Commercial sale or deposition in a public library or website is prohibited.

TABLE 1. The statistics (Min, Max and Mean±SE) of 27 morphometric characters measured for different species of the genus *Odontobuthus* . The results of one-way ANOVA have been presented in the last column. *,significant difference, (P<0.05).

	O. doriae (n=20)			*O. bidentatus* (n=9)			*O. tirgari* (n=6)			Kruskall-Wallis
	Min	Max	Mean±S.E.	Min	Max	Mean±S.E.	Min	Max	Mean±S.E.	P<
BL	66.01	76.31	71.123±0.622	70.8	82.24	73.600±1.530	58.12	74.17	66.131±2.581	0.05
CL	8.21	10.00	9.055±0.091	8.64	9.71	9.223±0.117	7.32	9.14	7.971±0.251	0.05
CWP	9.57	11.00	10.214±0.090	9.55	10.8	10.374±0.130	8.71	10.39	9.290±0.268	0.05
CWA	5.65	6.75	6.164±0.066	5.88	6.62	6.234±0.070	5.15	6.11	5.481±0.133	0.05
X	3.00	3.82	3.349±0.053	3.27	3.66	3.474±0.045	2.92	3.57	3.145±0.095	0.05
Y	5.21	6.31	5.759±0.061	5.31	6.21	5.774±0.102	4.41	5.55	4.870±0.157	0.05
CHL	13.44	15.92	14.452±0.152	13.12	16.78	15.303±0.373	13.13	15.02	13.976±0.253	0.05
ML	4.52	5.48	5.073±0.056	4.50	5.47	4.997±0.109	4.00	4.72	4.211±0.112	0.05
MFL	9.70	11.36	10.441±0.097	10.83	12.22	11.413±0.144	9.74	11.55	10.573±0.236	0.05
Mt(I)L	5.00	6.00	5.490±0.070	5.28	6.48	5.618±0.122	4.35	5.87	5.141±0.216	n.s.
Mt(I)H	4.25	5.21	4.660±0.064	4.23	5.12	4.858±0.096	3.85	5.09	4.331±0.183	0.05
Mt(I)W	5.08	6.50	5.718±0.085	5.50	6.44	5.992±0.104	4.62	6.27	5.388±0.227	0.05
Mt(II)L	5.69	7.26	6.383±0.086	6.19	7.38	6.594±0.128	4.95	6.64	5.926±0.243	0.05
Mt(II)H	3.94	5.08	4.485±0.072	4.23	4.91	4.612±0.081	3.54	5.00	4.100±0.196	0.05
Mt(II)W	4.67	5.90	5.229±0.075	4.90	5.67	5.355±0.087	4.09	5.30	4.631±0.171	0.05
Mt(III)L	6.07	7.18	6.668±0.075	6.43	7.71	6.926±0.131	5.29	6.78	6.068±0.230	0.05
Mt(III)H	3.92	4.86	4.388±0.061	4.20	4.92	4.524±0.079	3.48	4.77	3.976±0.174	0.05
Mt(III)W	4.30	5.58	4.819±0.075	4.34	5.21	4.887±0.088	3.74	4.78	4.143±0.148	0.05
Mt(IV)L	7.26	8.80	7.871±0.095	7.89	8.88	8.252±0.105	6.48	7.74	7.176±0.197	0.05
Mt(IV)H	3.56	4.88	4.105±0.077	3.70	4.52	4.085±0.086	3.14	4.12	3.460±0.139	0.05
Mt(IV)W	4.06	5.12	4.513±0.062	4.20	4.88	4.586±0.070	3.67	4.68	3.996±0.145	0.05
Mt(V)L	7.00	10.30	9.307±0.155	9.24	10.83	9.876±0.155	7.89	9.37	8.708±0.208	0.05
Mt(V)H	3.00	3.60	3.307±0.035	3.11	3.75	3.491±0.069	2.81	3.48	3.101±0.100	0.05
Mt(V)W	4.31	5.68	5.110±0.075	4.88	5.71	5.228±0.108	4.09	5.20	4.465±0.157	0.05
TIL	7.34	9.00	8.242±0.082	8.00	9.14	8.606±0.139	6.70	7.64	7.171±0.131	0.05
TIW	3.53	4.35	3.928±0.050	4.14	4.75	4.393±0.063	3.15	4.08	3.493±0.126	0.05
TIH	3.31	4.00	3.659±0.041	3.82	4.41	4.118±0.072	3.00	3.64	3.261±0.096	0.05

Paratypes: Khorasan Razavi Province: 1♀, 1♀ subadult, 9 juv. ZMFUM, 1♂1♀ FKCP, Gonabad, ca.3 Km Northeast of Kakhk, Marghesh vill., 34.146 °N, 58.644 °E, 1 September 2007, leg. O. Mirshamsi (ZMFUM-scr-2121 to ZMFUM-scr-2130); 1♂, 7♀ subadult, 15 juv. ZMFUM, Gonabad, ca.3 Km Northeast of Kakhk, Marghesh vill., 34.146 °N, 58.644 °E, 15 July 2011, leg. O. Mirshamsi & S. Azghadi, (ZMFUM-scr-2091 to ZMFUM-scr-2115); 3♀, 4♀ subadult, 1♂ subadult, ZMFUM, Gonabad, Northeast of Kakhk, Ostad road, 34.125° N, 58.775° E, 6 August 2011, leg. O. Mirshamsi & S. Azghadi (ZMFUM-scr-2131 to 2138); 1♂1♀1♀ subadult, AMNH, Khorasan Prov., Gonabad, ca. 3 Km Northeast of Kakhk, Marghesh vill., 34.146 °N, 58.644°E, 1 September 2012, leg. O. Mirshamsi.

Etymology: The species name is a patronym honoring Prof. Siavash Tirgari, for his contributions to the study of scorpions in Iran.

Diagnosis: Scorpions of medium to large size (Figs. 4–5), ranging from 60 to 72 mm in males and 66 to 75 mm in females; General coloration yellow to yellowish green; ocular tubercle located on anterior half of prosoma with following index: 0.65±0.025; dentate margins of fixed and movable fingers of pedipalps with 12–13 rows of oblique denticles; longer movable finger relative to the manus length (MFL/ML 1.88–2.66); ventrosubmedian

TERMS OF USE
This pdf is provided by Magnolia Press for private/research use.
Commercial sale or deposition in a public library or website is prohibited.

carinae of metasomal segments II–III with three to five pairs of distinct denticles; anterior ventral margin of metasomal segment IV with transverse row of eight or more enlarged granules; Metasomal segment IV L/W 1.80±0.128; ventrolateral carinae of metasomal segment V with three strong lobate denticles; Lateral anal arch armed with two strong and one minor lobe; posterior ventral margin of metasomal segment V with six reduced lobes; smaller and narrower telson (TlL/W 2.06±0.142; TlL/H 2.20±0.151).

TABLE 2. PCA for species of the genus *Odontobuthus*. The values of four principal components for each morphometrics and the percent of explained variance by each component are presented.

Components	PC_1	PC_2	PC_3	PC_4
Initial Eigenvalues	0.0241	0.0015	0.0012	0.00094
Total % of variance	77.963	4.860	3.773	3.043
BL	-0.1488	0.08104	-0.3338	0.1154
CL	-0.1895	-0.1648	0.02517	0.08021
CWP	-0.1524	-0.1045	0.06705	0.02035
CWA	-0.1712	-0.1674	-0.00527	0.03655
X	-0.1706	0.09809	0.08947	-0.1032
Y	-0.2092	-0.3106	-0.09085	0.1741
CHL	-0.1356	0.2475	-0.05057	-0.02955
ML	-0.2106	-0.3688	-0.2281	0.1263
MFL	-0.1009	0.4259	0.05719	0.02878
Mt(I)L	-0.1648	0.1579	-0.338	-0.079
Mt(I)H	-0.188	0.1001	0.06441	-0.2554
Mt(I)W	-0.1993	0.2049	-0.00345	-0.2201
Mt(II)L	-0.1791	0.1022	-0.3497	-0.03122
Mt(II)H	-0.2189	0.0297	0.08087	-0.3433
Mt(II)W	-0.221	0.006302	-0.08418	-0.09614
Mt(III)L	-0.1793	0.0557	-0.325	0.1184
Mt(III)H	-0.206	-0.01727	0.1564	-0.2134
Mt(III)W	-0.244	-0.1022	-0.07238	-0.1119
Mt(IV)L	-0.1753	0.1008	-0.1919	0.1436
Mt(IV)H	-0.2578	-0.3066	0.08102	-0.2169
Mt(IV)W	-0.2089	-0.1031	0.1285	-0.1517
Mt(V)L	-0.1746	0.2813	-0.1566	0.08588
Mt(V)H	-0.1659	0.1099	0.1932	-0.0521
Mt(V)W	-0.2189	-0.1753	0.2821	-0.04082
TlL	-0.1579	-0.1326	0.05084	0.5191
TlW	-0.2377	0.1795	0.3151	0.2895
TlH	-0.2242	0.232	0.3414	0.3796

Other Iranian *Odontobuthus* species are distinguishable from *O. tirgari* sp. nov. by the following main characteristics:

O. doriae: Scorpions of medium size ranging from 66 to 76.31 mm in total length; X/Y index 0.582±0.036; dentate margins of fixed and movable fingers of pedipalps with 13–14 rows of oblique denticles (MFL/ML 2.06±0.089); ventrosubmedian carinae of metasomal segments II–III with three pairs of very strong denticles; anterior ventral margin of metasomal segment IV with transverse row of four large denticles; lateral anal arch with two distinct enlarged denticles; telson indices TlL/W 2.10±0.139, TlL/H 2.25±0.127.

O. bidentatus: Scorpions of medium size ranging from 70.8 to 82.24 mm in total length; X/Y index 0.60±0.026; dentate margins of fixed and movable fingers of pedipalps with 13–14 rows of oblique denticles

TERMS OF USE
This pdf is provided by Magnolia Press for private/research use.
Commercial sale or deposition in a public library or website is prohibited.

(MFL/ML 2.29±0.12); ventrosubmedian carinae of metasomal segments II–III with two enlarged denticles; anterior ventral margin of metasomal segment IV with transverse row of eight large denticles; lateral anal arch with three distinct enlarged denticles; posterior ventral margin of metasomal segment V with four reduced lobes; telson indices TlL/W 1.96±0.086, TlL/H 2.09±0.112.

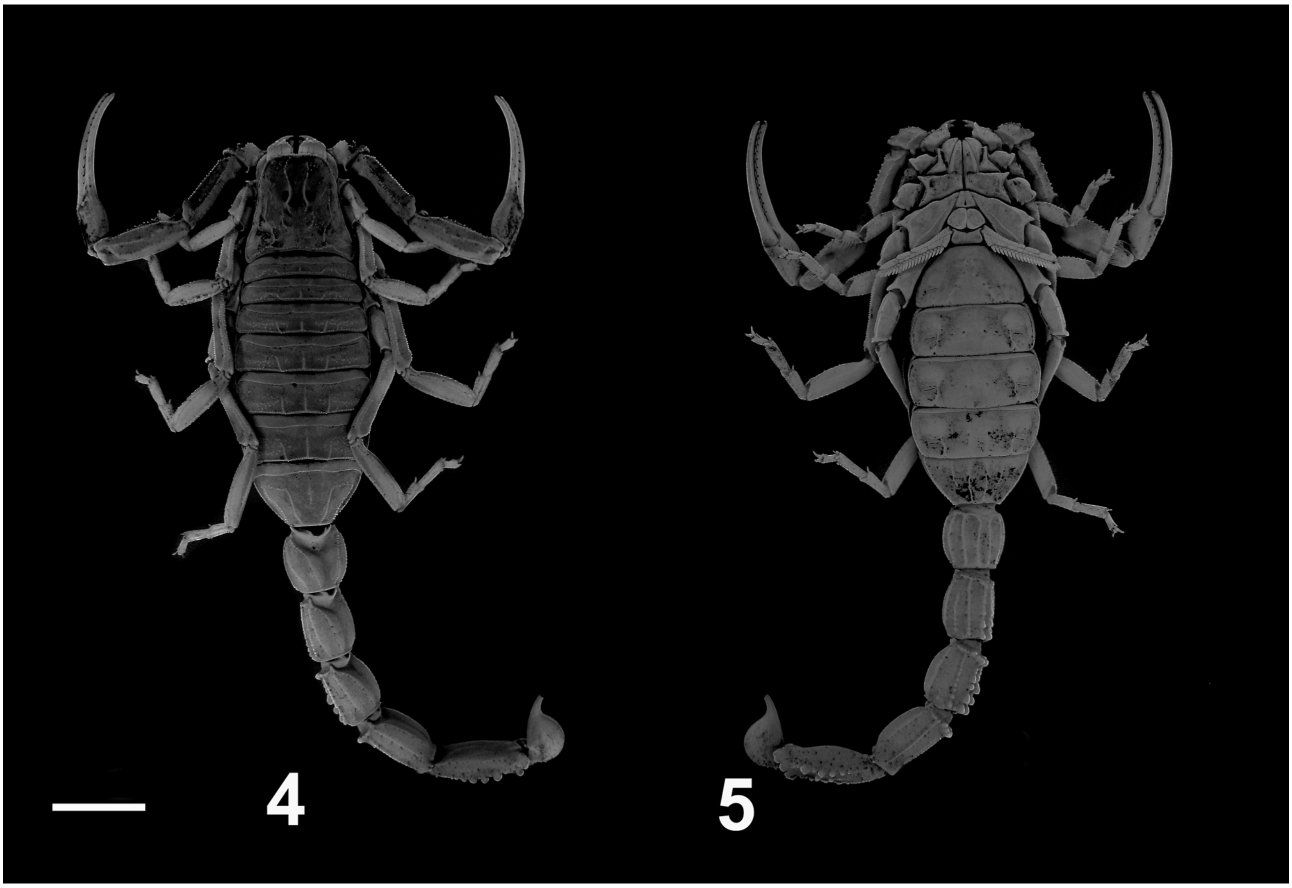

FIGURES 4–5. *Odontobuthus tirgari* sp. nov. female holotype. Habitus viewed under UV fluorescence. 1) dorsal and 2) ventral aspects. Scale bar: 10 mm.

Description of female holotype:

Measurements of holotype female (mm): BL: 74.17; CL: 9.14; CWP: 10.39; CWA: 6.11; X: 3.57; Y: 5.55; CHL: 15.02; ML: 4.72; MFL: 11.55; Mt(I)L: 5.87; Mt(I)H: 5.09; Mt(I)W: 6.27; Mt(II)L: 6.64; Mt(II)H: 5.00; Mt(II)W: 5.30; Mt(III)L: 6.78; Mt(III)H: 4.77; Mt(III)W: 4.78; Mt(IV)L: 7.73;Mt(IV)H: 4.12; Mt(IV)W: 4.68; Mt(V)L: 9.37; Mt(V)H: 3.48; Mt(V)W: 5.20; TlL: 7.11; TlW: 4.08; TlH: 3.64.

Coloration **(Figs. 8–9)** Almost brownish-yellow; with dark pigmentation under median and lateral eyes; without color patterns or markings on mesosoma; Pedipalps and legs slightly lighter than body and without color patterns; ventral surface slightly lighter than dorsal; metasoma yellow.

Carapace **(Figs. 4, 14, 24)** Trapezoid shaped, wider than long (CWA/CL:0.67; CWP/CL: 1.14); intercarinal surfaces of prosoma finely granular; anterior margin of prosoma moderately emarginated; prosoma carination well developed, central lateral, and posterior median carinae completely aligned; anterior median carinae moderately granular; central median, posterior median and central lateral carinae granular; anteromedian sulcus shallow; posteromedian sulcus shallow and wide; posterolateral furrow wide and curved; ocular tubercle located on anterior half of prosoma (X/CL: 0.39; X/Y=0.64); distance between median eyes twice ocular diameter; three pairs of lateral eyes.

TERMS OF USE
This pdf is provided by Magnolia Press for private/research use.
Commercial sale or deposition in a public library or website is prohibited.

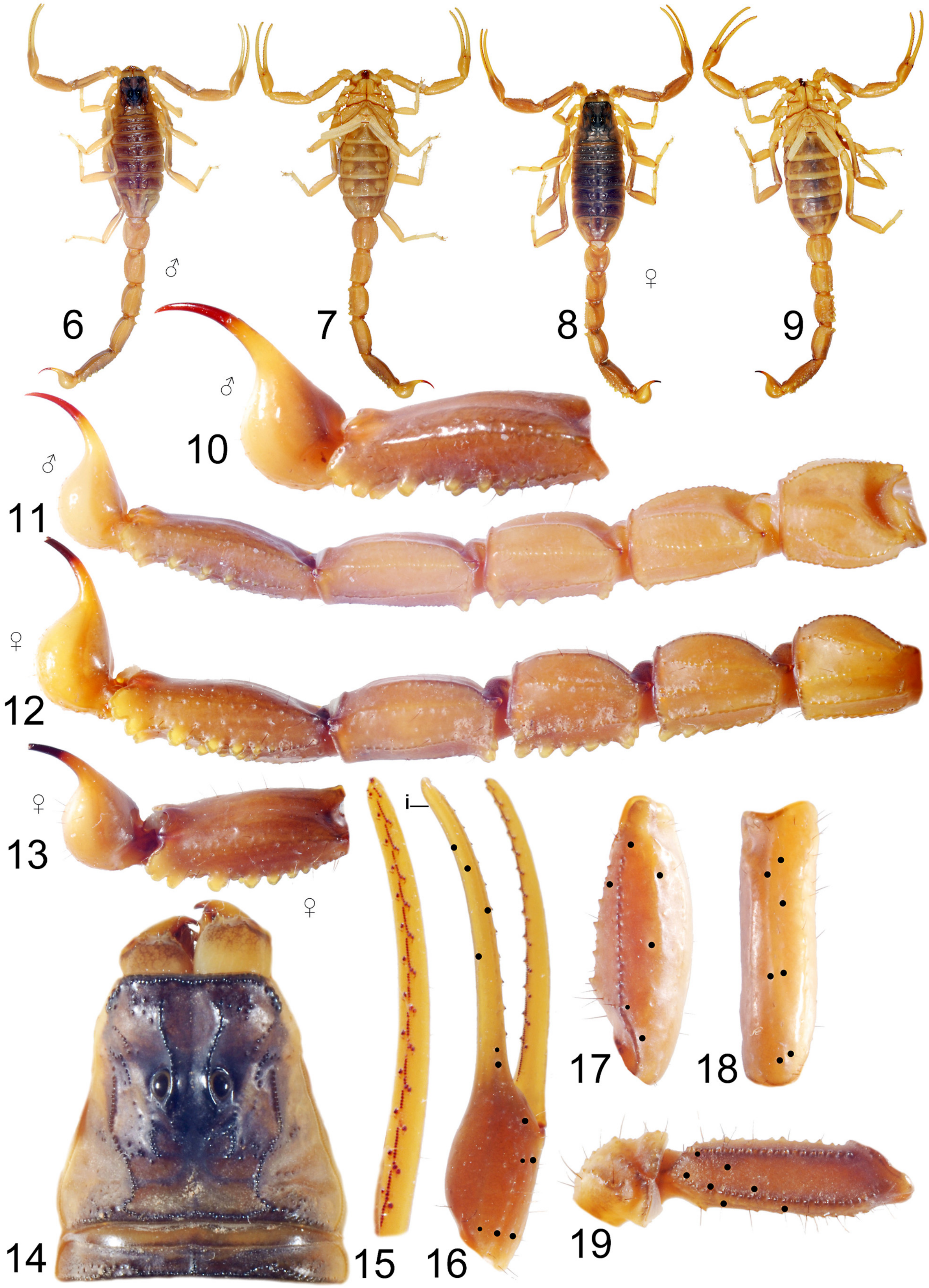

FIGURES 6–19. *Odontobuthus tirgari* sp. nov. 6) dorsal habitus of male paratype; 7) ventral habitus of male paratype; 8) dorsal habitus of female paratype; 9) ventral habitus of female paratype; 10) lateral view of telson and fifth metasomal segment of male paratype; 11) lateral view of metasoma in male paratype; 12) lateral view of metasoma in female paratype; 13) lateral view of telson and fifth metasomal segment of female paratype; 14) prosoma carination of female paratype; 15) fixed finger of chela of female paratype; 16) lateral view of chela of female paratype; 17) dorsal aspect pedipalp patella of female paratype; 18) external aspect of pedipalp patella of female paratype; 19) dorsal aspect of pedipalp femur of female paratype.

TERMS OF USE
This pdf is provided by Magnolia Press for private/research use.
Commercial sale or deposition in a public library or website is prohibited.

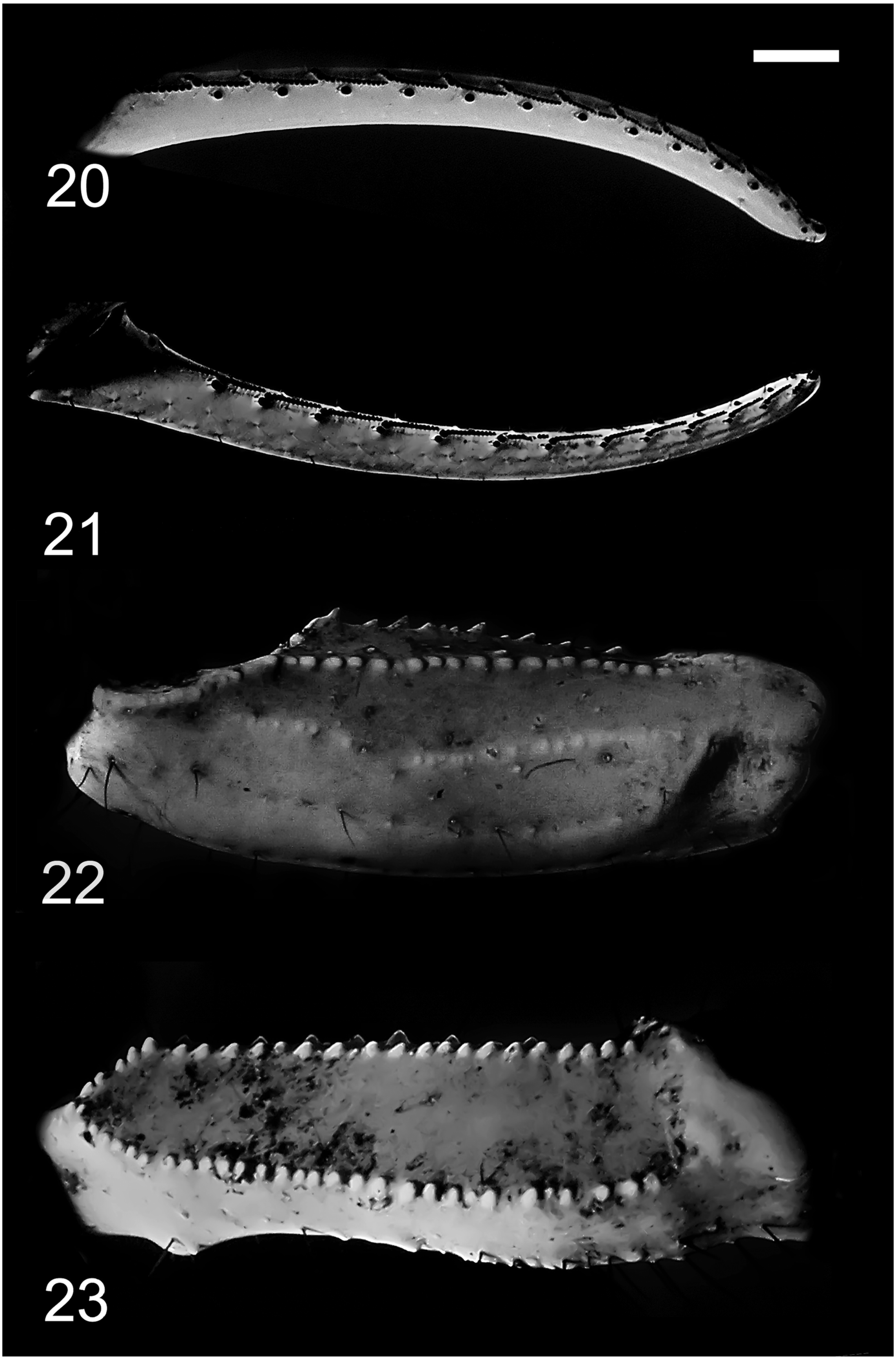

FIGURES 20–23. *Odontobuthus tirgari* sp. nov. female holotype under UV fluorescence. 20) Pedipalp fixed finger; 21) Pedipalp movable finger; 22) dorsal aspect of pedipalp patella; 23) dorsal aspect of pedipalp femur. Scale bar:

TERMS OF USE
This pdf is provided by Magnolia Press for private/research use.
Commercial sale or deposition in a public library or website is prohibited.

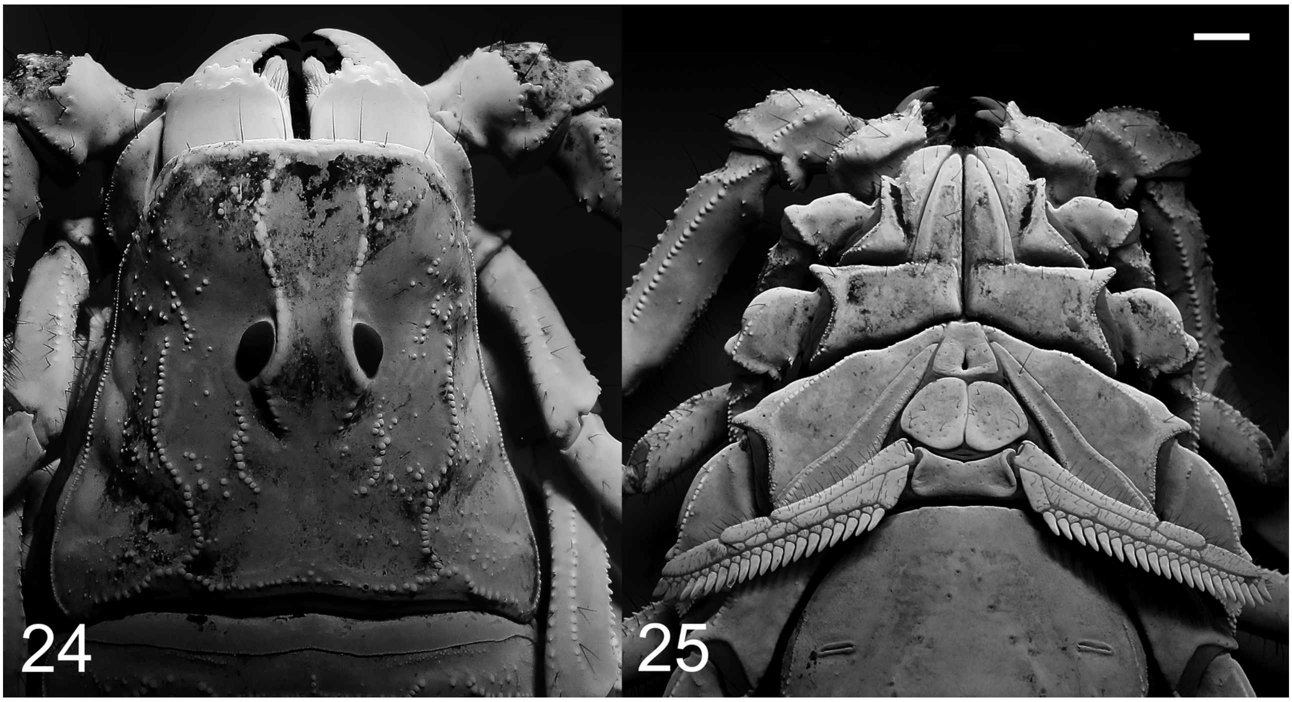

FIGURES 24–25. *Odontobuthus tirgari* sp. nov. female holotype under UV fluorescence.24) prosoma carination; 25) coxosternal area. Scale bar: 1 mm.

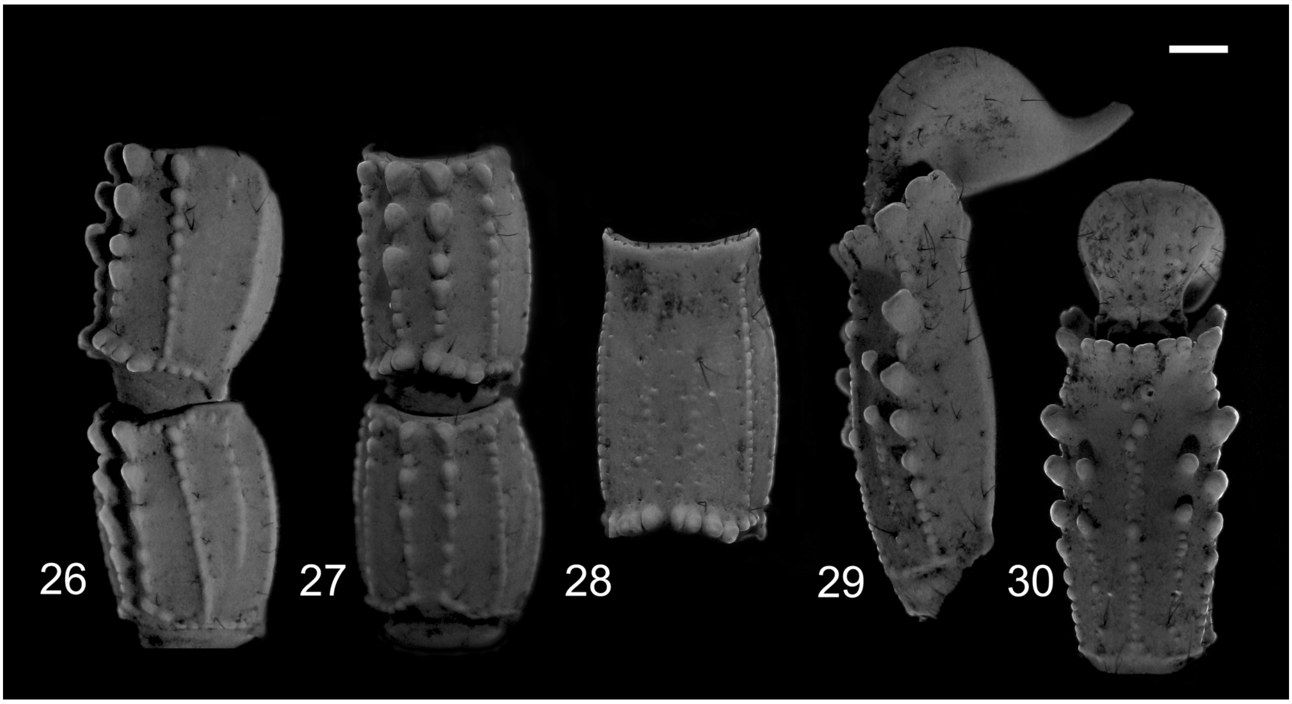

FIGURES 26–30. *Odontobuthus tirgari* sp. nov. female holotype under UV fluorescence. 26) lateral aspect of metasomal segments II and III; 27) ventral aspect of metasomal segments II and III; 28) ventral aspect of metasomal segment IV; 29) lateral aspect of metasomal segment V and telson; 30) ventral aspect of metasomal segment V and telson. Scale bar: 1 mm.

Chelicerae with two basal denticles on ventral aspect of fixed finger; movable finger with equally sized external and internal distal denticles.

Mesosoma **(Figs. 5, 8–9, 25)** Tergites I–VI tricarinate; tergite VII pentacarinate with lateral pairs strongly serratocrenulate; median carinae on tergite VII incomplete, present on anterior half and weakly granulate; intercarinal surface of tergites finely granular; sternites III–VI without carinae; sternite VII with four moderately

TERMS OF USE
This pdf is provided by Magnolia Press for private/research use.
Commercial sale or deposition in a public library or website is prohibited.

developed carinae, the lateral carinae present on anterior half of segment; pectines not extend beyond the coxa-trochanter joint of the leg IV; with three marginal and eight median lamellae; fulcra present; pectinal teeth present along the entire posterior margin of each pectine; pectinal tooth count 20|19; sternum type I sub-pentagonal and slightly wider than long with a deep median depression; genital operculum completely divided longitudinally with fine, short bristles.

Legs Ventral surface of tarsi with two rows of fine setae; legs III–IV with tibial spurs; with bifurcate prolateral pedal spurs.

Metasoma **(Figs. 12–13, 26–30)** Segment I decacarinate; segment II–IV octocarinate; lateral inframedian carinae incomplete and present only on posterior half of segment II–III; lateral inframedian carinae of segment III with three separate granules; all carinae on segments I–III moderately to strongly granular; ventral carinae on segments II–III strongly dentate with three to five distinct posterior rounded denticles; carinae on segment IV weakly to moderately granular; anterior ventral margin of segments III–IV with six large and rounded denticles; segment V pentacarinate; ventrolateral carinae on segment V strongly dentate with large rounded posterior denticles; ventral posterior margin of metasomal segment V with six distinct denticles; lateral anal arch with two large and one smaller lobes.

Telson **(Figs. 12–13, 29–30)** Oblong-ovoid, with dorsal surface flat (TlH/TlL: 0.51; TlW/TlL: 0.57); ventral surface of telson smooth; not wider than the metasomal segment V (TlW/Mt(V)W: 0.78).

Pedipalps **(Figs. 15–23)** all segments relatively long. *Femur*: 3.5 times longer than wide with four complete granular carinae; dorsoexternal, dorsointernal and ventrointernal carinae strongly granular; internal carinae weakly developed with five separate dentate granules; intercarinal surfaces smooth; *Patella*: 2.75 times longer than wide; dorsointernal carinae strong, dorsomedian carinae, dorsoexternal carinae, external, ventroexternal, and ventromedian carinae weakly to moderately developed; *Chela*: manus not wider than patella; fingers relatively long, 2.3 times longer than manus; primary denticle subrows (including proximal subrow): fixed finger, 13 right, 13 left; movable finger13 right, 13 left; all oblique rows of denticles expect proximal flanked by external and internal accessory granules; movable finger with five subdistal granules, two internal and three external; trichobothrium *et* adjacent to the proximal end of denticle subrow 8; *est* adjacent to denticle subrow 9.

Trichobothriotaxy **(Figs. 16–19)** Orthobothriotaxic type Aβ, with following segment totals: femur, 11 (5 dorsal, 4 internal, 2 external), patella, 13 (5 dorsal, 1 internal, 7 external) and chela, 15 (8 manus, 7 fixed finger); in total 39 trichobothria per pedipalp; trichobothria *esb, Esb, Eb3, d2* (patella) and *d2* (femur) petite.

Description of male paratype (ZMFUM-scr-2121)

Measurements of male paratype (mm): BL: 66.45; CL: 7.19; CWP: 8.18; CWA: 5.07; X: 2.27; Y: 4.5; CHL: 13.37; ML: 4.27; MFL: 9.82; Mt(I)L: 6.18; Mt(I)H: 4.10; Mt(I)W: 5.49; Mt(II)L: 6.65; Mt(II)H: 4.15; Mt(II)W: 4.74; Mt(III)L: 7.05; Mt(III)H: 4.00; Mt(III)W: 4.22; Mt(IV)L: 8.00; Mt(IV)H: 3.48; Mt(IV)W: 3.89; Mt(V)L: 9.43; Mt(V)H: 3.10; Mt(V)W: 4.00; TlL: 8.00; TlW: 3.25; TlH: 3.11.

Coloration as described for female holotype.

Carapace **(Fig. 31)** trapezoid shaped; wider than long (CWA/CL: 0.70; CWP/CL: 1.13); intercarinal surfaces of prosoma finely granular; anterior margin of prosoma moderately emarginated; prosoma carination well developed; central lateral and posterior median carinae completely aligned; anterior median carinae strongly granular; central median, posterior median and central lateral carinae serratocrenulate; anteromedian sulcus deep and narrow; posteromedian sulcus shallow and wide; posterolateral furrow wide and curved; ocular tubercle located on anterior half of prosoma (X/CL: 0.32; X/Y: 0.50); distance between median eyes twice ocular diameter; three pairs of lateral eyes.

Chelicerae as described for female holotype.

TERMS OF USE
This pdf is provided by Magnolia Press for private/research use.
Commercial sale or deposition in a public library or website is prohibited.

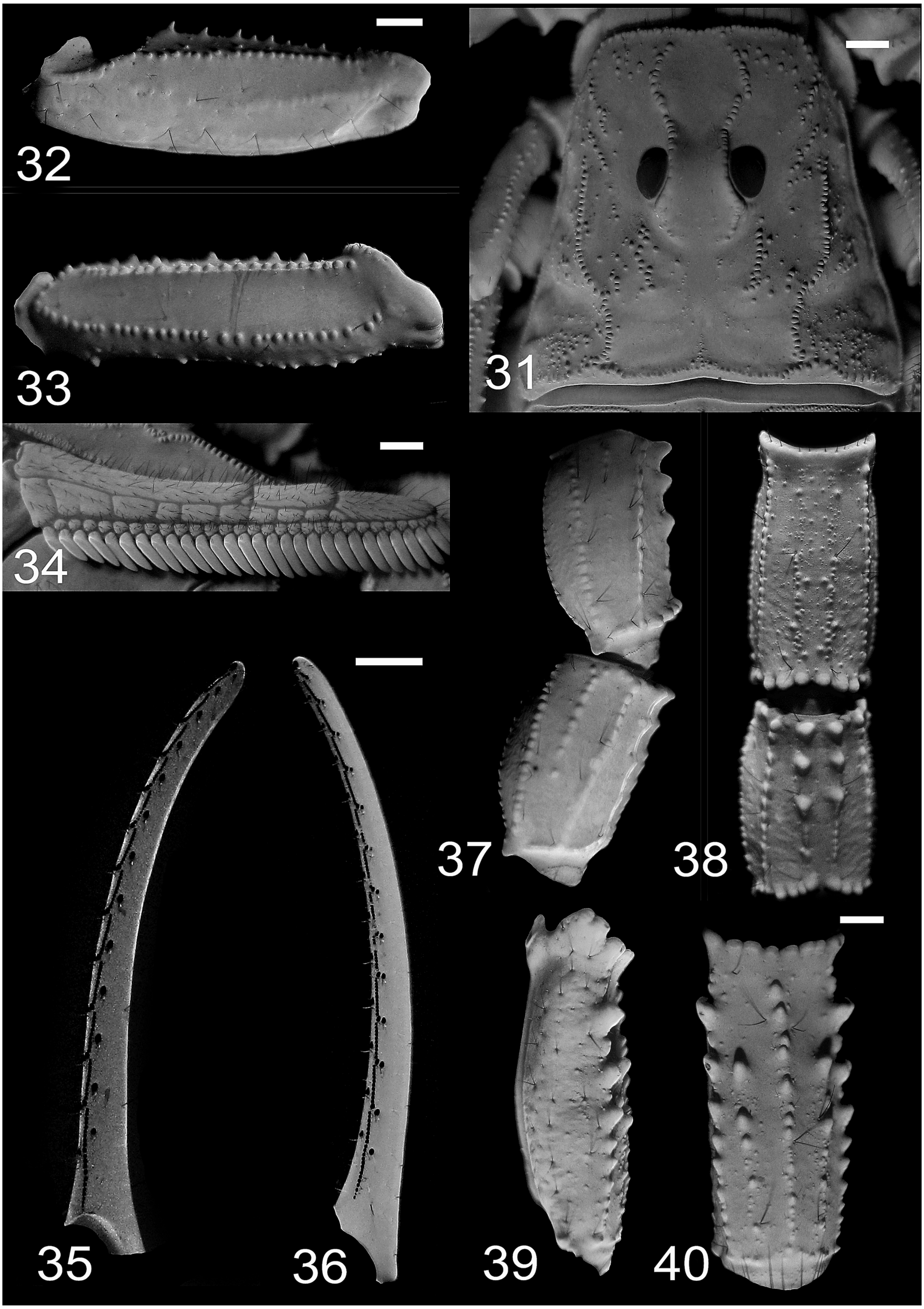

FIGURES 31–40. *Odontobuthus tirgari* sp. nov. male paratype under UV fluorescence. 31) prosoma carination; 32) dorsal aspect of pedipalp patella; 33) dorsal aspect of pedipalp femur; 34) left pectine; 35) fixed finger of chela; 36) movable finger of chela; 37) lateral aspect of metasomal segments II–III; 38) ventral aspect of metasomal segments III–IV; 39) lateral aspect of metasomal segment V; 40) ventral aspect of metasomal segment V. Scale bar= 1mm.

TERMS OF USE
This pdf is provided by Magnolia Press for private/research use.
Commercial sale or deposition in a public library or website is prohibited.

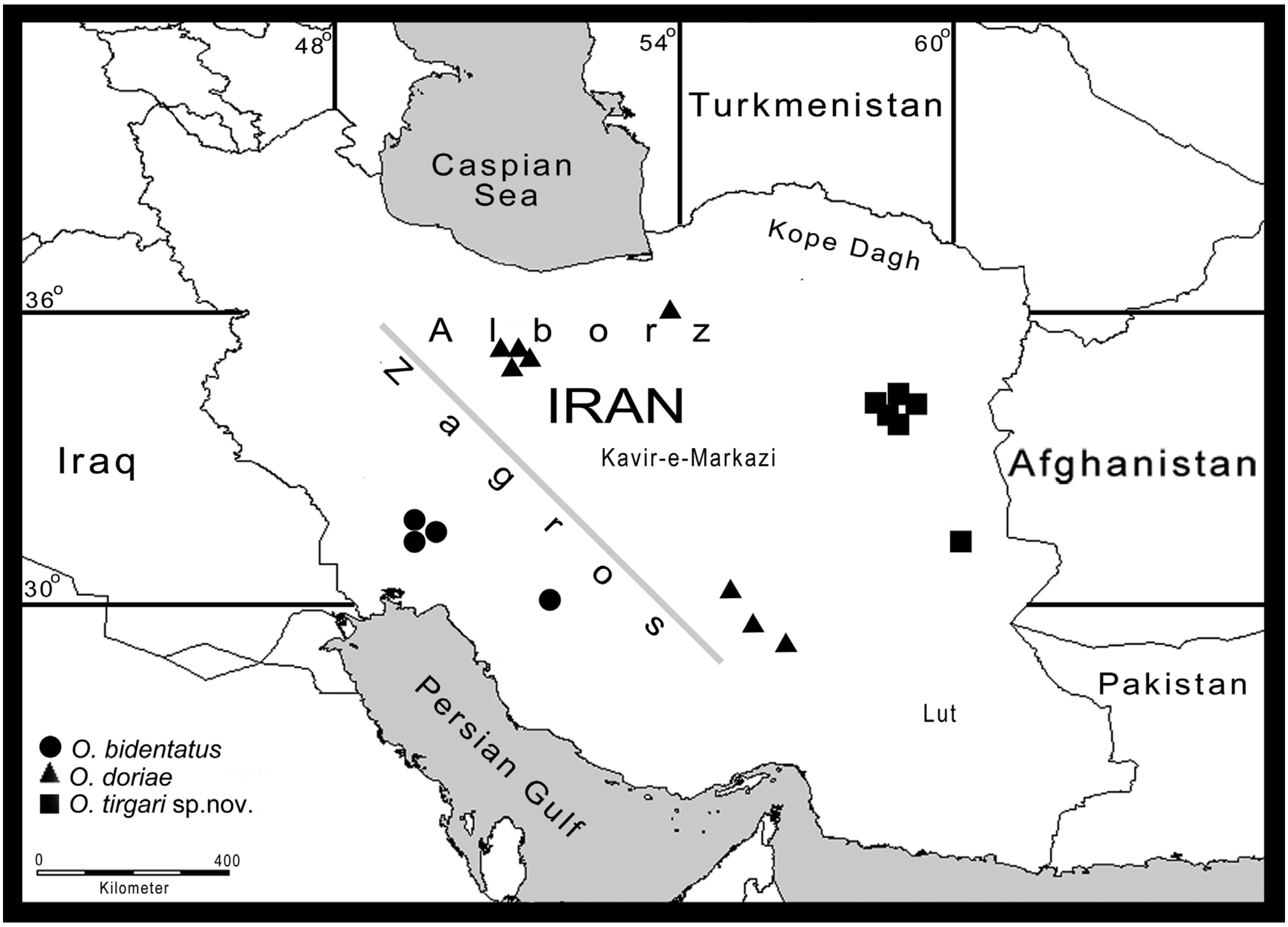

FIGURE 41. Map of the distribution of *O. doriae, O. bidentatus* and *O. tirgari* sp. nov. specimens used in morphological and molecular studies.

Mesosoma tergites I–VI tricarinate; tergite VII pentacarinate with lateral pairs strongly serratocrenulate; median carinae on tergite VII incomplete and weakly granular; intercarinal surfaces of tergites coarsely granular; sternites III–VI without carinae; sternite VII with four weakly granular carinae; the lateral carinae on sternite VII present on anterior half of the segment; pectines extend beyond the coxa-trochanter joint of leg IV; with three marginal and ten middle lamellae; fulcra present; pectinal teeth present along the entire posterior margin of each pectine (Fig. 34); pectinal tooth count 31|30; sternum type I, subpentagonal and longer than wide with a median depression; genital operculum completely divided longitudinally.

Legs as described for female holotype.

Metasoma **(Figs. 37–40)** segment I decacarinate; segments II–IV octocarinate; lateral inframedian carinae incomplete and present only on posterior half of segment II; lateral inframedian carinae on segment III with three weak posterior granules; all complete carinae on metasomal segments I–IV weakly to moderately granular; ventral carinae on segments II and III dentate with three distinct pairs of short triangular granules; anterior margins of segments III and IV with six rounded granules; segment V pentacarinate; ventrolateral carinae strongly dentate with large triangular posterior denticles; ventral posterior margin with six distinct denticles; lateral anal arch with two large and one smaller lobes.

Telson **(Figs. 10–11)** Oblong-ovoid, longer and narrower than female with dorsal surface flat (TlH/TlL: 0.38; TlW/TlL: 0.40); ventral surface of telson weakly granular; not wider than the metasomal segment V (TlW/Mt(V)W: 0.81).

Pedipalps **(Figs. 32–33, 35–36)** all segments relatively long; Femur: 3.76 times longer than wide with four complete granular carinae; dorsoexternal, dorsointernal and ventrointernal carinae serratocrenulate; internal carinae weakly developed with several separate pointed granules; intercarinal surfaces smooth; Patella: 3.37 times

TERMS OF USE
This pdf is provided by Magnolia Press for private/research use.
Commercial sale or deposition in a public library or website is prohibited.

longer than wide; with eight complete carinae; dorsointernal carinae moderately granular; dorsomedian, dorsoexternal, external, ventroexternal and ventromedian carinae weakly developed and smooth; ventrointernal carinae strong, dentate granulate; internal carinae strong, with several pointed granules, including the proximal patella spur; Chela: not wider than patella; fingers relatively long, 2.23 times longer than manus; primary denticle subrows (including proximal subrow): fixed finger, 12 right, 12 left; movable finger 12 right, 12 left; all oblique rows of denticles expect proximal flanked by external and internal accessory granules; movable finger with six subdistal granules, two internal and four external; trichobothrium *et* adjacent to the denticle subrow 7; *est* adjacent to denticle subrow 9.

Trichobothriotaxy as described for female holotype.

Discussion

The results of the current study increase the number of Iranian species of the scorpion genus *Odontobuthus* to three namely, *O. doriae*, *O. bidentatus* and *O. tirgari* sp. nov. The species, which is described here, is the fifth species in this genus. The results of Kruskall-Wallis ANOVA and multivariate analyses provide further indication of morphological differentiation among the three Iranian *Odontobuthus* species: *O. doriae*, *O. bidentatus* and *O. tirgari* sp. nov. Comparison of morphometric variables in *O. tirgari* sp. nov. mainly highlight the larger median eyes index (X/Y), longer movable fingers relative to the manus length, narrower metasomal segment IV and smaller telson. Moreover, the plots of PCA (Fig. 1) and CDA (Fig. 2) provide evidence of morphological differentiation of *O. tirgari* sp. nov., respectively.

Maximum likelihood and Bayesian analyses of the mitochondrial *COI* sequence data presented here strongly support the genetic differentiation and the monophyly of *O. doriae* and *O. bidentatus*, and provide additional support for raising the eastern Iranian populations of *Odontobuthus* to the species level (Fig. 3). Notably, genetic divergence between *O. tirgari* and other species is similar to that observed between *O. doriae* and *O. bidentatus* (i.e. 11% mtDNA sequence divergence).

The species of the genus *Odontobuthus* display an allopatric or parapatric geographic distribution in India, Pakistan, Iran, Iraq and northern Oman (Lowe, 2010). The species *O. doriae* is found on the eastern foothills of the Zagros Mountains, southern foothills of Elburz Mountains, and mountains of western Iran and the central Iranian Plateau; *O. bidentatus* is found in the Tigris-Euphrates River drainage of eastern Iraq and western foothills of the Zagros Mountains in Iran; and *O. tirgari* sp. nov. is endemic to low elevations of the eastern Iranian Plateau (Fig. 41). This fragmented geographical distribution corresponds to the Miocene/Pliocene paleoclimatic and geomorphological vicariance events, which may have been responsible for affecting species distributions in the Iranian Plateau (Lowe 2010). These include the collision of the Arabian Plate with the Eurasian Plate (11–9 Mya) and the uplifting and formation of Zagros orogeny accompanied by sinking of the central and eastern parts of Iranian Plateau (5–3 Mya) (Macey et al., 1998; Rastegar-Pouyani, 2006; Rastegar-Pouyani et al., 2010; Lowe, 2010, Mirshamsi et al, 2010). However, our *COI*-based phylogenetic topology is compatible with *O. doriae* ancestral to *O. tirgari* sp. nov. and *O. bidentatus*. Nevertheless, having low nodal support for the *O. tirgari*+ *O. bidentatus* Clade (i.e. 72%) we will not discuss more about the temporal order of the *Odontobuthus* species in the Iranian Plateau. This observation is open to testing by detailed molecular phylogenetic analyses using multiple mitochondrial and nuclear genes and more intensive sampling.

Acknowledgements

The authors thank Ghasem M. Kashani and Elham Tavakkoli for their help during field activities. We also thank Lorenzo Prendini (AMNH) and two anonymous reviewers for their helpful critical comments on an earlier version of the manuscript. The financial supports were provided by office of research affairs, Ferdowsi University of Mashhad (Project no. 2/15248) and the Iran National Science Foundation (INSF- 90001780), which are gratefully acknowledged.

TERMS OF USE
This pdf is provided by Magnolia Press for private/research use.
Commercial sale or deposition in a public library or website is prohibited.

References

Aliabadian, M., Nijman, V., Mahmoudi, A., Naderi, M., Vonk, R. & Vences, M. (in press) ExCaliBAR: a simple and fast software utility to calculate intra- and interspecific distances from DNA barcodes. *Contributions to Zoology.*

Birula, A.A. (1900) Beiträge zur Kenntniss der Scorpionen fauna Ost-Persiens (1. Beiträg). *Bulletin de l'Académie Impériale des Sciences de St.-Pétersbourg, Sér.* 5, 12, 355–375.

Birula, A.A. (1905) Beiträge zur Kenntniss der Skor-pionenfauna Persiens (3. Beiträge). *Bulletin de l'Académie Impériale des Sciences de St. Pétersbourg, Sér.* 5, 23, 119–148.

Farzanpay, R. (1987) *Knowing scorpions*. No. 312, Biology 4, Central University Publications, Teheran, 231 pp. [in Farsi with Latin index]

Folmer, O., Black, M., Hoeh, W., Lutz, R. & Vrijenhoek, R. (1994) DNA primers for amplification of mitochondrial cytochrome c oxidase subunit I from diverse metazoan invertebrates. *Molecular Marine Biology and Biotechnology*, 3, 294–299.

Hammer, A., Harper, D.A.T. & Ryan, P.D. (2001) PAST: Paleontological statistics software package for education and data analysis. *Palaeontologia Electronica*, 4, 1–9.

Kovařík, F. (1997) Results of the Czech Biological Expedition to Iran. Part 2. Arachnida: Scorpiones, with descriptions of *Iranobuthus krali* gen. n. et sp. n. and *Hottentotta zagrosensis* sp. n. (Buthidae). *Acta Societatis Zoologicae Bohemicae*, 61, 39–52.

Lamoral, B.H. (1979) The scorpions of Namibia. *Annals of the Natal Museum*, 23, 497–784.

Lourenço, W.R. & Pézier, A. (2002) Taxonomic consideration of the genus *Odontobuthus* Vachon (Scorpiones, Buthidae), with description of a new species. *Revue suisse de Zoologie,* 109, 115–125.

Lowe, G., Kutcher, S.R. & Edwards, D. (2003) A powerful new light source for ultraviolet detection of scorpions in the field. *Euscorpius*, 8, 1–7.

Lowe, G. (2010) A New Species of *Odontobuthus* (Scorpiones: Buthidae) from Northern Oman. *Euscorpius*, 96, 1–22.

Macey, J.R., Schulte, J.A., Ananjeva, N.B., Larson, A., Rastegar-Pouyani, N., Shammakov, S.M. & Papenfuss, T.J. (1998) Phylogenetic relationships among agamid lizards of the *Laudakia caucasia* species group: testing hypotheses of biogeographic fragmentation and an area cladogram for the Iranian Plateau. *Molecular Phylogenetics and Evolution,* 10, 118–131.
http://dx.doi.org/10.1006/mpev.1997.0478

Mirshamsi, O., Sari, A., Elahi, E. & Hosseinie, S. (2010) Phylogenetic relationships of *Mesobuthus eupeus* (C.L. Koch, 1839) inferred from *COI* sequences (Scorpiones: Buthidae). *The Journal of Natural History*, 44, 2851–2872.
http://dx.doi.org/10.1080/00222933.2010.512400

Navidpour, S., Fet, V., Kovařík, F. & Soleglad, M.E. (2008a) Scorpions of Iran (Arachnida, Scorpiones). Part III. Ilam Province. *Euscorpius*, 69, 1–29.

Navidpour, S., Kovařík, F., Soleglad, M.E. & Fet, V. (2008b) Scorpions of Iran (Arachnida, Scorpiones). Part I. Khoozestan Province. *Euscorpius*, 65, 1–41.

Navidpour, S., Kovařík, F., Soleglad, M.E. & Fet, V. (2008c) Scorpions of Iran (Arachnida, Scorpiones). Part IV. Kohgilouyeh & Boyer Ahmad Province. *Euscorpius*, 74, 1–24.

Navidpour, S., Soleglad, M.E., Fet, V. & Kovařík, F. (2008d) Scorpions of Iran (Arachnida, Scorpiones). Part II. Bushehr Province. *Euscorpius*, 67, 1–33.

Pocock, R.I. (1897) Descriptions of some new species of scorpions from India. *Journal of the Bombay Natural History Society*, 11, 102–117.

Pocock, R.I. (1900) Arachnida. *In*: Blanford, W.T. (Ed.), *The Fauna of British India, including Ceylon and Burma*. Published under the authority of the Secretary of State for India in Council. Taylor and Francis, London, xii & 279 pp.

Posada, D. & Crandall, K.A. (1998) MODELTEST: testing the model of DNA substitution. *Bioinformatics,* 14, 817–818.
http://dx.doi.org/10.1093/bioinformatics/14.9.817

Prendini, L. (2004) Systematics of the Genus *Pseudolychas* Kraepelin (Scorpiones: Buthidae). *Annals of the Entomological Society of America,* 97, 37–63.
http://dx.doi.org/10.1603/0013-8746(2004)097[0037:sotgpk]2.0.co;2

Rastegar-Pouyani, N. (2006) *Systematics of the genus Assacus (Sauria: Gekkonidae) on the Zagros Mountains, Iran. Paper presented at: Herpetologia Bonnensis II*. Proceedings of the 13th Congress of the Societas Europaea Herpetologica; October 2005; Germany, 117–120.

Rastegar Pouyani, E., Rastegar Pouyani, N., Kazemi Noureini, S., Joger, U. & Wink, M. (2010) Molecular phylogeny of the *Eremias persica* complex of the Iranian plateau (Reptilia: Lacertidae), based on mtDNA sequences. *Zoological Journal of the Linnean Society*, 158, 641–660.
http://dx.doi.org/10.1111/j.1096-3642.2009.00553.x

Ronquist, F. & Huelsenbeck, J.P. (2003) MRBAYES 3: Bayesian phylogenetic inference under mixed models. *Bioinformatics*, 19, 1572–1574.
http://dx.doi.org/10.1093/bioinformatics/btg180

Rozas, J., Sanchez-DelBarrio, J.C., Messeguer, X. & Rozas, R. (2003) DnaSP, DNA polymorphism analyses by the coalescent and other methods. *Bioinformatics,* 19, 2496–2497.
http://dx.doi.org/10.1093/bioinformatics/btg359

TERMS OF USE
This pdf is provided by Magnolia Press for private/research use.
Commercial sale or deposition in a public library or website is prohibited.

Simon, C., Frati, F., Beckenbach, A., Crespi, B., Liu, H. & Flook, P. (1994) Evolution, weighting, and phylogenetic utility of mitochondrial gene sequences and a compilation of conserved polymerase chain reaction primers. *Annals of the Entomological Society of America,* 87, 651–701.

Sissom, W.D. (1990) Systematics, biogeography and paleontology. *In*: Polis, G.A. (Ed.), *Biology of Scorpions.* Stanford University Press, Stanford, California, pp. 64–160.

Stahnke, H.L. (1970) Scorpion nomenclature and mensuration. *Entomological News,* 81, 297–316.

Tamura, K., Dudley, J., Nei, M. & Kumar, S. (2007) MEGA4: Molecular Evolutionary Genetics Analysis (MEGA) software version 4.0. *Molecular Biology and Evolution,* 24, 1596–1599.
http://dx.doi.org/10.1093/molbev/msm092

Thompson, J.D., Gibson, T.J., Plewniak, F., Jeanmougin, F. & Higgins, D.G. (1997) The ClustalX windows interface: flexible strategies for multiple sequence alignment aided by quality analysis tools. *Nucleic Acids Research*, 24, 4876–4882.
http://dx.doi.org/10.1093/nar/25.24.4876

Thorell T. (1876) Études scorpiologiques. *Atti della Società italiana di scienze naturali Genova*, 19, 75–272.

Volschenk, E. (2005) A new technique for examining surface morphosculpture of scorpions. *The Journal of Arachnology,* 33, 820–825.
http://dx.doi.org/10.1636/s03-047.1

Appendix A

Comparative material examined: ***Odontobuthus doriae*** **: Tehran Province:** 28♀, 2♂, ca. 15 km Southeast of Tehran, 35.696° N, 51.423° E, 30 May 2011, leg. Sh. Navidpour (ZMFUM-scr-2001 to ZMFUM-scr-2030); 1♂ im, Varamin, Ghale boland vill., 35.321° N, 51.650° E, 27 October 2008, leg. Gh.M Kashani (ZMFUM-scr-2038); **Semnan Province:** 2♀, Semnan, Desret Research Center, 35° 35.415 N, 053° 26.783E, 1 August 2009, leg. O. Mirshamsi (ZMFUM-scr-2031, 2032); **Kerman Province:** 1♀, Bardsir-Sirjan road, 29.946° N, 56.552°, 19 June 2009, leg. Sh. Navidpour (ZMFUM-scr-2039); 1♂ im., Shahre Babak, Estabragh, 30.470 °N, 59.093° E, 19 June 2009, leg. Sh. Navidpour (ZMFUM-scr-2040); 1♂ im, Shahre Babak, Marza, 30.028° N, 55.094° E, 19 June 2009, leg. Sh. Navidpour (ZMFUM-scr-2041).

Odontobuthus bidentatus**: Khoozestan Province:** 11♀, 2♂, Omidiyeh, 30.963° N, 49.529° E, 23 March 2007, leg. Sh. Navidpour (ZMFUM-scr-2061 to ZMFUM-scr-2073).

Identification key for the genus *Odontobuthus*

1. Anal arch with two lateral lobes.. . . . . *O. doriae* (Thorell, 1876)
- Anal arch with three lateral lobes 2
2. Ventral carinae of third metasomal segment with two pairs of denticles . . . . . . *O. bidentatus* Lourenço & Pézier, 2002.
- Ventral carinae of third metasomal segment with three or more pairs of denticles 3
3. Ventral anal arch with two enlarged triangular denticles . . . . *O. brevidigitus* Lowe, 2010
- Ventral anal arch without two enlarged triangular denticles 4
4. Movable finger of pedipalp with 12–13 oblique rows of granules; Metasomal segment IV with transverse row of eight or more enlarged granules. . . . . *O. tirgari* sp. nov.
- Movable finger of pedipalp with 10–11 oblique rows of granules; metasomal segment IV with transverse row of six or fewer enlarged granules. . . . . *O. odonturus*